2 February 2001

ELSEVIER

Chemical Physics Letters 334 (2001) 18–23

CHEMICAL PHYSICS LETTERS

www.elsevier.nl/locate/cplett

Hydrogen Raman shifts in carbon nanotubes from molecular dynamics simulation

S.J.V. Frankland *, D.W. Brenner

Department of Materials Science and Engineering, Campus Box 7907, North Carolina State University, Raleigh, NC 27695-7907, USA

Received 13 March 2000; in final form 1 December 2000

Abstract

Shifts in Raman peak position relative to the gas-phase vibrational frequency have been calculated for molecular hydrogen in individual single-shell carbon nanotubes and nanotube ropes using a semiclassical model. The calculations predict that isolated hydrogen molecules inside of nanotubes have a Raman frequency that increases with nanotube size for radii less than about 2 nm, while intercalated hydrogen frequencies are independent of nanotube size. The model indicates that shifts in Raman frequencies could be used experimentally to distinguish between hydrogen inside and intercalated between nanotubes. © 2001 Elsevier Science B.V. All rights reserved.

1. Introduction

Fullerene nanotubes have been proposed as hydrogen storage media for vehicular fuel cell applications [1]. They are expected to provide a safe alternative to compressed or liquefied fuels. However, it is not clear how much hydrogen can be stored in carbon nanotube samples. Dillon et al. [1] measured ~5–10 wt% and ~50 kg/m^3 which is close to the target values of 6.5 wt% and 62 kg/m^3 recommended by the DOE Hydrogen Plan [2]. As the authors note [1], these values exceed the amount predicted by simple analysis of packing molecular hydrogen inside the nanotube, and they further propose additional external and interstitial adsorption. Nutzenadel et al. [3] subsequently reported 0.39 wt% for samples with a few percent multi-wall nanotubes and indicate the possibility of larger amounts of hydrogen stored in pure nanotube samples. Ye et al. [4] measured up to 8.25 wt% at low temperature (80 K) and high pressure. One of the highest reports is 14 wt% and 112 kg/m^3 observed at 313 K for the catalytic storage of hydrogen in potassium-doped nanotubes [5].

Computational studies have addressed issues relating to hydrogen adsorption in nanotubes [6–13], including the amount of hydrogen that can be stored [14–19]. Optimal conditions for storage have generally been found to include high pressures and/or low temperatures, and larger than van der Waals separations between the nanotubes due to swelling induced by the intercalated species [14–19]. Amounts lower than the target values are typically reported for ambient conditions [14,15,18,19].

A key remaining issue is the primary location of hydrogen within nanotube samples. Is hydrogen stored primarily on the inside of nanotubes, intercalated between nanotubes, external to the

* Fax: +1-919-515-7724.
E-mail address: sjvf@eos.ncsu.edu (S.J.V. Frankland).

PII: S0009-2614(00)01454-8

sample or possibly in impurities? From simulation it has been shown that either internal or intercalated hydrogen is feasible [17].

The Raman peak position of a hydrogen molecule is expected to be sensitive to its local environment. Therefore, Raman peak shifts could potentially be used to help identify hydrogen positions within nanotube samples. To explore this possibility, we have used a semiclassical model to predict qualitative trends in hydrogen Raman shifts relative to the gas-phase vibrational frequency for single hydrogen molecules within and between bundled nanotubes of various radii. The model uses classical dynamics to sample the surroundings of a hydrogen molecule in different environments. Relative Raman shifts are estimated from the energy difference in each environment between the ground and first excited vibrational state of the hydrogen molecule that arise from changes in hydrogen bond length and molecular polarizability.

Results for three different environments are presented: a hydrogen molecule inside a single nanotube, a hydrogen molecule inside one nanotube of a nanotube bundle, and a hydrogen molecule intercalated within a nanotube bundle (Fig. 1). For hydrogen inside of nanotubes, the model predicts a red-shifted Raman peak with a value that increases (i.e., a decreasing shift magnitude) with increasing nanotube radius. Intercalated hydrogen is predicted to have a broader Raman peak with a frequency not strongly dependent on nanotube radius. Hence, the model predicts that the Raman signal from a hydrogen molecule inside a nanotube is distinct from an intercalated molecule.

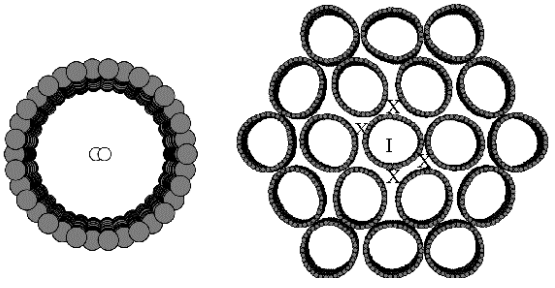

Fig. 1. The simulated systems. Left: individual carbon nanotube. Right: cluster of 19 nanotubes with hydrogen inside the tubes (I) and in four intercalated locations marked with an X.

2. Theoretical method

The model used to estimate hydrogen Raman shifts in this work is adapted from a study of C–H stretches of cyclohexane [20]. In this model changes in both the average bond length during vibration and the associated molecular polarizability are taken into account. The shift is modeled as the difference in the potential interactions between the nanotubes and the hydrogen molecule in the ground $(v = 0)$ and first excited $(v = 1)$ vibrational states. The hydrogen molecule is treated as a rigid rotor with the two vibrational states assigned different sets of carbon–hydrogen Lennard-Jones (LJ) 12–6 potential parameters. The environment of the hydrogen molecule is sampled by numerically integrating classical equations of motion for the hydrogen molecule described by its ground state LJ parameters interacting with the nanotube. The excited state parameters are then instantaneously applied to each configuration of the ground state trajectory so that the Raman shift during the trajectory is given as

$$\Delta v = U^{\mathrm{CH}}\left(\varepsilon^1, \sigma^1\right) - U^{\mathrm{CH}}\left(\varepsilon^0, \sigma^0\right), \tag{1}$$

where U^{CH} is a LJ 12–6 carbon–hydrogen potential, σ^0 and ϵ^0 represent the ground state parameters, and σ^1 and ϵ^1 represent the excited state parameters. The Raman shifts presented are averaged over the trajectory.

The LJ parameters for hydrogen in the $v = 1$ state are given by $\sigma^1 = \sigma^0 + \Delta\sigma$ and $\epsilon^1 = \epsilon^0 + \Delta\epsilon$, where $\Delta\sigma$ and $\Delta\epsilon$ account for the difference in bond length and polarizability, respectively, of the hydrogen molecule in the two vibrational states. The quantity $\Delta\sigma$ is estimated from the harmonic and anharmonic force constants of the H_2 vibration using the relation [21,22].

$$\Delta\sigma = \Delta r/2 = \frac{hcvf}{4k^2}, \tag{2}$$

where Δr is the change in bond length of the hydrogen molecule, h is Planck's constant, c the speed of light, v the hydrogen vibrational frequency, k the

harmonic force constant, and f the cubic anharmonicity. The force constant k is obtained from the H_2 vibrational frequency. From Oxtoby [23] the value for the cubic anharmonicity is

$$f = \frac{-3\omega_e^2}{2B_e r_e^3}\left(1 + \frac{\alpha_e \omega_e}{6B_e^2}\right), \tag{3}$$

where ω_e is the vibrational frequency at infinitesimal amplitude, B_e the rotational constant, α_e the rotation–vibration interaction constant, and r_e the bond distance. Using the values $v = 4160.2\ \mathrm{cm}^{-1}$, $\omega_e = 4395\,\mathrm{cm}^{-1}$, $\alpha_e = 2.993\,\mathrm{cm}^{-1}$, $B_e = 60.80\,\mathrm{cm}^{-1}$, and $r_e = 0.7416 \times 10^{-8}$ cm [24], yields a $\Delta\sigma$ value of 0.029 Å.

The percentage change in polarizability is estimated from the expression

$$\frac{\Delta\alpha}{\alpha} = \frac{\frac{\partial\alpha}{\partial r}\Delta r}{\alpha}, \tag{4}$$

where α is the mean polarizability of the hydrogen molecule and $\partial\alpha/\partial r$ is the polarizability derivative. The polarizability and polarizability derivative for H_2 are $\alpha = 0.87 \times 10^{-40}$ C m^2/V and $\partial\alpha/\partial r = 1.3 \times 10^{-30}$ C m/V from empirical and ab initio values reported by Gough et al. [25]. These values yield a polarizability change $\Delta\alpha$ of 4.3% per hydrogen. The resulting LJ parameters for hydrogen in each of the vibrational states as well as for carbon are given in Table 1. Carbon–hydrogen parameters are obtained using the Lorentz–Berthelot mixing rules [26].

In the cyclohexane study, changes in LJ parameters were fit to experimental Raman shifts for different fluid environments [20]. The inferred change in bond length was within 20% of experiment, and the polarizability change was within a factor of 2–3 of experiment. Although the nanotube environment in which the hydrogen sits is less isotropic than the previous fluid simulations, it is expected that the relative shifts will also have a similar accuracy and be within a factor of 2–3 of experiment, and that qualitative shift trends are predicted [1].

Table 1
Lennard-Jones parameters

Species	ε (K) [26]	σ (Å) [26]
H (each), $v = 0$	15.0	2.81
H (each), $v = 1$	15.6	2.84
C	51.2	3.35

The simulated hydrogen-nanotube systems are illustrated in Fig. 1. They are a hydrogen molecule inside an individual nanotube (Fig. 1, left), inside the center nanotube of a rope of 19 nanotubes (Fig. 1, right), and intercalated between nanotubes (Fig. 1, right). Nanotubes of various chirality were modeled. In each of these systems, periodic boundaries are used along the nanotube axis, yielding nanotubes of infinite length.

During the simulation, the hydrogen molecule was allowed to move around the inside of the nanotube or intercalated site. The translational dynamics and rigid rotor motion of the hydrogen molecule and the carbon atom dynamics were calculated by numerically integrating classical equations of motion with a third-order Gear algorithm using a timestep of 2 fs [26,27]. Intra-atomic interactions within the nanotubes were modeled by a bond-order potential [28,29] [2] used in previous nanotube simulations [30–32]. Interactions between bundled nanotubes were modeled with a LJ 12–6 potential using the parameters in Table 1. Nonbonded interactions within the same nanotube were neglected. To improve the sampling of hydrogen velocities, initial velocities were chosen from a Maxwell–Boltzmann distribution at the simulation temperature (100 K) each time the hydrogen entered a region near the center of the

[1] How reasonable is this expectation? Rare-gas clusters of H_2/Ar and H_2/Xe have Raman shifts of $-1.83\ \mathrm{cm}^{-1}$ and $-3.31\ \mathrm{cm}^{-1}$, respectively. Solutions of hydrogen in these gases have shifts of -9 to $-11\ \mathrm{cm}^{-1}$ (Ar) and $-21\ \mathrm{cm}^{-1}$ (Xe) [L.E.S. de Souza and D. Ben Amotz, J. Chem. Phys. 104 (1996) 139]. The mean polarizability per carbon atom of graphite is $\alpha = 1.6\ \mathrm{A}^3$, very similar to that of argon, $\alpha = 1.66\ \mathrm{A}^3$; compare [D. Nicholson, Surf. Sci. 181 (1987) L189] to [P.W. Atkins, Physical Chemistry, fifth ed., Freeman, New York, 1994]. Therefore, one could reasonably expect an intermediate value for the vibrational shifts of H_2 on a relatively flat nanotube. In this work, the shift reported for the largest and, therefore relative to the hydrogen, the flattest nanotube (Fig. 2) is $-16\ \mathrm{cm}^{-1}$, which is about 45% larger than the solution value for H_2/Ar.

[2] A slightly modified form of the potential in [29] is used for the present calculations [D.W. Brenner, O.A. Shenderova, S.B. Sinnott, J.A. Harrison, unpublished.]

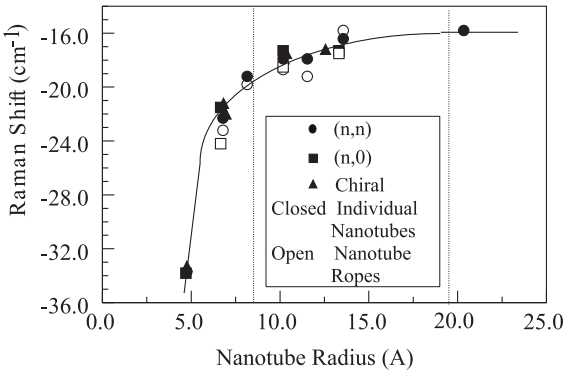

Fig. 2. Predicted Raman shift relative to a gas-phase molecule for a hydrogen molecule inside of a nanotube. Shown are data for hydrogen inside individual nanotubes (closed symbols) and in the center nanotube of a nanotube rope (open). The dotted lines mark the regions below which hydrogen is expected not to intercalate and above which the shift becomes independent of nanotube size for both internal and intercalated hydrogen. The solid line is to guide the eye.

nanotube or intercalate hole. Good statistics were obtained from run lengths of 100 ps for the individual nanotubes and 40–80 ps for the nanotube ropes. For the individual nanotubes, the first 10–20 ps were eliminated for equilibration of the shift trajectory. For the nanotube ropes, the shift trajectories were consistent after the first 2–10 ps.

3. Results and discussion

Plotted in Fig. 2 are predicted Raman shifts for hydrogen inside of a series of nanotubes as a function of nanotube radius. The data include 17 (n,n), $(n,0)$, and (n,m) individual nanotubes (closed symbols), and a total of eight bundles containing (n,n) and containing $(n,0)$ nanotubes (open symbols) [3]. The estimated maximum uncertainty of the averages reported is ± 2 cm^{-1} due to the finite timescale of the simulations. All of the Raman shifts are red indicating that the hydrogen is free to vibrate without compression. Predicted differences in shifts between the individual and bundled nanotubes are within the uncertainty of the calculations. Apparently the nanotube–nanotube interactions and the slight nanotube deformation observed in the simulated ropes (Fig. 1b) do not significantly affect the magnitude of the shifts. From Fig. 2 it is apparent that the chirality of the nanotubes also does not significantly affect the magnitude of the Raman shift.

In both the individual nanotubes and in the nanotube ropes, the primary trend for internal hydrogen is an increase in Raman frequency with an increase in nanotube size. At larger nanotube sizes the shift appears to reach a limiting value as the nanotube surface flattens out relative to the hydrogen. When the nanotubes are very small, the hydrogen begins to sense both sides of the nanotube producing a Raman shift of roughly double the size for the smallest nanotubes simulated. In between, there is the smoothly increasing trend of Raman frequency with nanotube size.

To model hydrogen intercalated between nanotubes, simulations were carried out with a hydrogen molecule placed in one of four symmetrically equivalent locations indicated by the X symbols in Fig. 1. The predicted relative Raman shifts as a function of nanotube radius are plotted in Fig. 3. The shifts for each site X indicated in Fig. 1 are shown in Fig. 3a and the averages per rope in Fig. 3b. Several things are evident from this data. First, the magnitude of the shifts for intercalated hydrogen are generally larger than those for internal hydrogen. Second, the smaller ropes ($r < 8$ Å) do not intercalate hydrogen well. The $(12,12)$ rope (the smallest one denoted in Fig. 3) has a significantly higher Raman frequency than the slightly larger $(21,0)$, and was unable to intercalate hydrogen in one of the four chosen sites. Neither the $(10,10)$ rope nor the $(17,0)$ rope (not shown in Fig. 3) were able to accommodate intercalated hydrogen. Third, the Raman shift is predicted to depend very strongly on the size and shape of the site containing the hydrogen. Fig. 3a shows the scatter in the shifts calculated for each of the locations shown in Fig. 1. Although symmetrically equivalent, the sites are inequivalent over the 40 ps simulation timescale because of

[3] The (n,m) notation refers to the chiral vector of the nanotube in terms of the primitive in-plane lattice vectors of a graphene sheet. For further details see [M.S. Dresselhaus, G. Dresselhaus, P.C. Eklund, Science of Fullerenes and Carbon Nanotubes, Academic Press, New York, 1996].

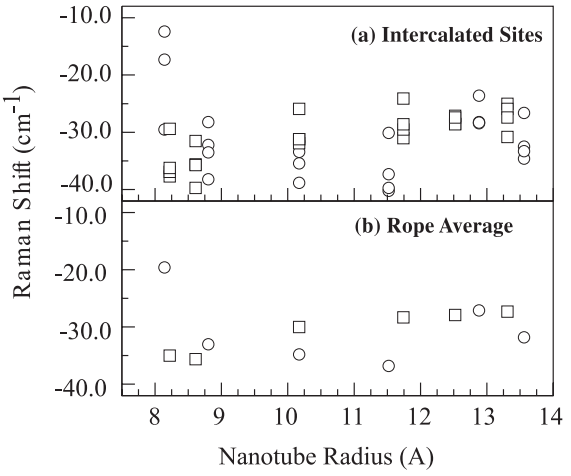

Fig. 3. Predicted Raman shift relative to a gas-phase molecule for a hydrogen molecule intercalated in a nanotube rope. The shifts per intercalated site X are shown in (a) and their averages per rope in (b). Circles are for (n,n) nanotubes, and squares $(n,0)$.

nanotube deformation. From the simulations it is unclear how long the deformation persists, though over experimental timescales the flexibility of the nanotubes is expected to yield a distribution of hole environments. This distribution of hydrogen environments will broaden the Raman band. Therefore, it is predicted that intercalated hydrogen molecules will have relatively broad Raman bands compared to internal hydrogen molecules. Finally, for the (n,n) ropes there is no significant trend in shift with nanotube size (Fig. 3b). For the $(n,0)$ ropes there may be a slight increase in peak frequency with nanotube size, though this increase is small compared to the internal hydrogen and may well be obscured by the broadening of the peak from the several environments represented. It is therefore unlikely that shifts arising from intercalated hydrogen molecules will show a consistent trend with nanotube size.

4. Conclusions

A semiclassical model was used to predict relative Raman shifts for a hydrogen molecule inside and between bundled nanotubes as a function of nanotube radius. These calculations lead to the following qualitative predictions for the relationship between the location of a hydrogen molecule and its Raman shift. First, Raman shifts for individual hydrogen molecules are expected to be red-shifted independent of the site at which the hydrogen resides. Second, if the hydrogen is internal to the nanotubes, the Raman peak frequency is expected to show an increase with nanotube radius. If the hydrogen is intercalated, broader bands will be observed with no frequency dependence on the nanotube size. These frequencies will be lower on average than those from internal hydrogen. Third, it is energetically unlikely for ropes of very small nanotubes ($r < 8$ Å) to intercalate hydrogen. Finally, for very large nanotubes ($r < 20$ Å), the Raman frequency is expected to be independent of nanotube size for either type of hydrogen. The cases examined here indicate that if both intercalated and internal hydrogen were present, the frequencies of the bands would be resolvable.

Acknowledgements

Helpful discussions with O.A. Shenderova, J.D. Schall, R. Superfine, O. Zhou, J.P. Lu, D. Srivastava, R. Jaffe, J. Glosli, P. Schmidt, and J. Pazik are gratefully acknowledged. This work is supported by a Multi-University Research Initiative of the Office of Naval Research through the North Carolina Center for Nanoscale Materials and the NASA-Ames Computational Nanotechnology Program.

References

[1] A.C. Dillon, K.M. Jones, T.A. Bekkedahl, C.H. Kiang, D.S. Bethune, M.J. Heben, Nature 386 (1997) 377.
[2] S. Hynek, W. Fuller, J. Bentley, Int. J. Hydrogen Energy 22 (1997) 601.
[3] C. Nutzenadel, A. Zuttel, D. Chartouni, L. Schlapbach, Electrochem. Solid State Lett. 2 (1999) 30.
[4] Y. Ye, C.C. Ahn, C. Witham, B. Fultz, J. Liu, A.G. Rinzler, D. Colbert, K.A. Smith, R.E. Smalley, Appl. Phys. Lett. 74 (1999) 2307.
[5] P. Chen, X. Wu, J. Lin, K.L. Tan, Science 285 (1999) 91.
[6] K.G. Ayappa, Chem. Phys. Lett. 282 (1998) 59.
[7] K.G. Ayappa, Langmuir 14 (1998) 880.

[8] I.A. Khan, K.G. Ayappa, J. Chem. Phys. 109 (1998) 4576.
[9] M.W. Maddox, K.E. Gubbins, Langmuir 11 (1995) 3988.
[10] G. Stan, M.W. Cole, J. Low Temp. Phys. 110 (1998) 539.
[11] G. Stan, M.W. Cole, Surf. Sci. 395 (1998) 280.
[12] I.V. Zaporotskova, A.O. Litinskii, L.A. Chernozatonskii, JETP Lett. 66 (1997) 840.
[13] D. Srivastava, Private communication.
[14] Q. Wang, J.K. Johnson, J. Phys. Chem. B 103 (1999) 277.
[15] Q. Wang, J.K. Johnson, J. Chem. Phys. 110 (1999) 577.
[16] V.V. Simonyan, P. Diep, J.K. Johnson, J. Chem. Phys. 111 (1999) 9778.
[17] F. Darkrim, D. Levesque, J. Chem. Phys. 109 (1998) 4981.
[18] M. Rzepka, P. Lamp, M.A. de la Casa-Lillo, J. Phys. Chem. B 102 (1998) 10894.
[19] P.A. Gordon, R.B. Saeger, Ind. Eng. Chem. Res. 38 (1999) 4647.
[20] S.J.V. Frankland, M. Maroncelli, J. Chem. Phys. 110 (1999) 1687.
[21] G.J. Remar, R.A. MacPhail, J. Chem. Phys. 103 (1995) 4381.
[22] D. Ben-Amotz, M.R. Lee, S.Y. Cho, D.J. List, J. Chem. Phys. 96 (1992) 8781.
[23] D.W. Oxtoby, Adv. Chem. Phys. 40 (1979) 1.
[24] G. Herzberg, Molecular Spectra and Molecular Structure, second ed., Van Nostrand, New York, 1950.
[25] K.M. Gough, M.M. Yacowar, R.H. Cleve, J.R. Dwyer, Can. J. Chem. 74 (1996) 1139.
[26] M.P. Allen, D.J. Tildesley, Computer Simulation of Liquids, Clarendon Press, Oxford, 1987.
[27] P.S.Y. Cheung, J.G. Powles, Mol. Phys. 30 (1975) 921.
[28] D.W. Brenner, O.A. Shenderova, D.A. Areshkin, in: K.B. Lipkowitz, D.B. Boyd (Eds), Reviews in Computational Chemistry, vol. 12, Wiley, New York, 1998, p. 207.
[29] D.W. Brenner, Phys. Rev. B 42 (1990) 9458.
[30] D.H. Robertson, D.W. Brenner, J.W. Mintmire, Phys. Rev. B 45 m (1992) 12592.
[31] D. Srivastava, D.W. Brenner, J.D. Schall, K.D. Ausman, M.F. Yu, R.S. Ruoff, J. Phys. Chem. B 103 (1999) 4330.
[32] A. Garg, J. Han, S.B. Sinnott, Phys. Rev. Lett. 81 (1998) 2260.